Digital Signal Processing and Artificial Intelligence for Automatic Learning

DLINE JOURNALS

ISSN:2583-5009

DSP 2026: 5 (4)
https://doi.org/10.6025/dspaial/2026/5/4/248-267

Spatial and Frequency-Band Characterization of EEG Signals During Motor Tasks: Electrode-Wise Analysis, Hemispheric Asymmetry, and Inter-Electrode Correlations

Yao-Liang Chung
National Taiwan Ocean University
Taiwan
ylchung@email.ntou.edu.tw

ABSTRACT

Electroencephalography (EEG) based brain computer interfaces (BCIs) require a clear understanding of how spectral activity is distributed across the scalp before discriminative features can be selected for motor task decoding. This study presents a spatial and frequency band characterization of exported EEG band power features recorded during two motor intention tasks, LeftRight and PullPush, using a 14-channel Emotiv headset (AF3, AF4, F3, F4, F7, F8, FC5, FC6, T7, T8, P7, P8, O1, O2). An archive of 102 valid CSV files containing theta, alpha, low beta, high beta and gamma features (70 features per file) was consolidated into 90 identifier task summaries, of which 43 identifiers contained both tasks and were retained for paired analysis. Because feature distributions exhibited extreme upper tail values, channel medians were used as robust summary statistics. Analyses comprised electrode wise and regional (frontal, frontocentral, temporal, parietal, occipital) profiling, paired Wilcoxon signed rank tests with Holm correction, log, (left/right) hemispheric asymmetry indices, and inter-electrode Spearman rank correlations. AF4 showed the highest median theta and alpha values in both tasks, while FC6 showed the highest median gamma; frontal sites dominated theta and alpha, and frontocentral sites dominated gamma. No electrode-wise or regional task contrast reached statistical significance after Holm correction. Laterality indices were consistently negative across all bands (median -0.65 to -0.46 in LeftRight; -0.62 to -0.41 in PullPush), and interelectrode correlations were predominantly positive (mean ρ= 0.565–0.701 and 0.570–0.665, respectively), with gamma most strongly correlated. These results provide a descriptive spatial spectral baseline, but indicate that exported band-power summaries alone do not establish reliable task discrimination or physiological lateralization. The findings motivate signal-quality verification, recovery of raw time series, and leakage controlled predictive validation before physiological or decoding claims are advanced.

Keywords: Electroencephalography (EEG), Brain Computer Interface (BCI), Motor Intention, Frequency-Band Analysis, Hemispheric Asymmetry, Inter Electrode Correlation, Emotiv EPOC, Spatial Spectral Characterization, Wilcoxon Signed-Rank Test, Feature Selection

Received: 2 April 2026, Revised: 5 July 2026, Accepted: 22 July 2026

Copyright: **DLINE**

1. Introduction

Brain computer interfaces (BCIs) establish a direct communication pathway between brain activity and external devices by translating neural signals into control commands. Electroencephalography (EEG) based BCIs have attracted substantial clinical and technological interest because EEG is non invasive, offers high temporal resolution, is comparatively portable, and can be implemented at relatively low setup cost. These characteristics make EEG based systems relevant to rehabilitation and assistive technologies, particularly for people with spinal cord injuries or limb nerve damage. Applications include robotic rehabilitation for individuals with motor impairments [2, 3], robotic arm control [4], gaming interfaces [5], and virtual reality control [6] .

Despite this potential, reliable EEG decoding remains challenging. Neural signals are nonstationary, high-dimensional, and heterogeneous, and their spectral characteristics can change in frequency and magnitude across tasks and states. Extracting discriminative information therefore requires attention to both frequency-specific activity and the spatial distribution of signals across electrodes. The present manuscript is framed around spatial and frequency-band characterization during motor tasks, with particular emphasis on electrode-wise patterns, hemispheric asymmetry, and inter electrode correlations.

2. EEG Signal Types and Their Relevance to BCI

EEG signals used in BCIs are commonly distinguished as evoked or spontaneous according to how they arise. Evoked potentials are elicited by external stimuli and include steady state visual evoked potentials (SSVEPs) and P300 potentials [7-10]. Spontaneous EEG, by contrast, reflects cortical activity associated with internal mental processes and does not require an external stimulus. Examples include slow cortical potentials (SCPs) and motor imagery (MI). The reviewed literature indicates that research on spontaneous EEG has placed particular emphasis on MI, whereas SCP-based BCIs remain comparatively underdeveloped [11, 12].

Motor-related EEG is especially important for assistive control because neural activity associated with movement preparation, imagined movement, and execution may provide information about intended actions. Alpha rhythms, typically described as occupying approximately 8–12 Hz, are prominent over posterior regions and are associated with attention and visual processing. The mu rhythm is an alpha-range rhythm over sensorimotor regions and is closely associated with movement preparation and execution. These observations motivate examining spectral bands together with the electrodes and cortical regions from which the signals are recorded.

2.1 Spatial, Spectral, and Connectivity Features in Prior Research

2.2 Frequency-specific and electrode-wise characteristics

Prior work suggests that the contribution of EEG frequency bands may vary with the motor task and the neural region under investigation. Studies of hand movement decoding have considered wrist movement [13, 14, 15], upper limb movement [Úbeda, A.], and elbow and shoulder movement [16]. Li et al. used EEG connectivity features to decode voluntary right hand movement and reported sensitivity in delta, theta, and gamma components recorded from electrodes over the premotor and somatosensory motor cortex [15]. Úbeda examined the feasibility of decoding upper limb kinematics from EEG during center out reaching movements [17]. Together, these studies support the relevance of examining frequency band contributions in relation to electrode location and specific motor behaviors.

Frequency selection has also been investigated directly in motor imagery decoding. J. V. Juan [18] examined the effects of EEG frequency bands on decoding pedaling motor imagery in four healthy volunteers, using a frequency band ablation study on recordings collected during static and pedaling motor imagery [18]. The study highlights the potential value of frequency specific analysis for identifying neural correlates of different mental states and optimizing feature selection for BCI applications. In related work, Shang presented a motor-imagery EEG feature extraction and classification approach based on wavelet threshold denoising [19].

2.3 Joint modeling of spectral and spatial information

EEG contains complementary spectral and spatial information, but extracting fine grained discriminative

features remains difficult. In the context of emotion recognition, Li developed the Spectral Convolution–Spatial Differential Transformer (SC-SDT), a framework that combines convolutional operations and a transformer architecture to model spectral and spatial characteristics jointly [20]. Although the application differs from motor-task decoding, this work illustrates the broader methodological interest in integrating multiple domains of EEG information rather than relying on isolated features.

Related challenges arise in EEG-based assessment of neurological and developmental conditions. EEG signals are heterogeneous and nonstationary, and methods that use only single-domain features or static graph representations may not fully capture changing neural interactions. To address these limitations for automated autism spectrum disorder (ASD) detection, M. Das proposed an EEG-based functional brain-network framework incorporating graph learning [21]. This line of work underscores the importance of considering relationships among electrodes alongside individual-channel characteristics. However, findings from ASD detection should not be treated as direct evidence of performance in motor task decoding; rather, they provide methodological context for connectivity aware EEG analysis. [22, 23].

2.4 Research Motivation and Focus

The literature reviewed here covers EEG-based BCI applications, frequency band analysis, motor imagery decoding, movement related EEG connectivity, and models that combine spectral and spatial information. These studies indicate that useful information may be distributed across frequency bands, electrodes, and inteelectrode relationships. Nevertheless, the reviewed material also points to the continuing challenge of characterizing these dimensions in a coherent way for motor task EEG analysis.

Accordingly, the stated focus of this work is the spatial and frequency band characterization of EEG signals during motor tasks. The analysis is organized around three related dimensions: (i) electrode-wise variation in EEG characteristics, (ii) hemispheric asymmetry, and (iii) correlations between electrodes. Examining these dimensions together can provide a structured description of how spectral activity is distributed across recording sites and how electrode-level patterns relate to one another. The supplied material does not specify the dataset, participant characteristics, preprocessing pipeline, statistical procedures, or empirical findings; these details should be added from the actual study before the manuscript is presented as a complete research article.

EEG-based BCIs offer a non-invasive route for translating neural activity into commands for assistive and interactive systems. Existing research demonstrates the relevance of motor imagery, movement related frequency bands, electrode location, and connectivity features, while broader EEG studies highlight the value of jointly modeling spatial and spectral information. Building on this background, electrode wise characterization, hemispheric asymmetry analysis, and inter electrode correlation analysis provide complementary perspectives for investigating motor task EEG. A complete journal submission should connect this motivation to a clearly specified dataset and reproducible methods, then report results that directly address these analytical dimensions.

2.5 Research Statement

This study aims to provide a comprehensive spatial and frequency band characterization of Electro-encephalography (EEG) signals during distinct motor intention tasks (Left Right and Pull Push). By systematically analyzing electrode wise variations, hemispheric asymmetry, and inter electrode correlations, this research seeks to map the distribution of spectral activity (Theta, Alpha, Beta, and Gamma bands) across the scalp. The ultimate goal is to establish a robust statistical and spatial foundation for Brain Computer Interface (BCI) applications, identifying how exported frequency band features vary across recording sites and informing future feature selection, leakage controlled predictive validation, and explainable machine learning models for motor task decoding.

2.6 Research Problem

Despite the potential of EEG-based BCIs in assistive and rehabilitation technologies, reliable decoding of motor intentions remains challenging due to the nonstationary, high-dimensional, and heterogeneous nature of neural signals. Relying on isolated spatial or spectral features often fails to capture the complex neural interactions underlying motor tasks.

Specifically, this research addresses the following core problems:

1. Spatial-Spectral Distribution: How do EEG frequency-band power features (Theta, Alpha, Beta, Gamma) distribute across specific electrode locations and broader cortical regions (frontal, frontocentral, temporal, parietal, occipital) during distinct motor tasks?

2. Task-Specific Discriminability: Are there statistically significant differences in electrode-wise or regional EEG feature magnitudes between Left-Right and Pull-Push motor tasks after correcting for multiple comparisons?

3. Hemispheric Asymmetry: Is there a systematic left-right hemispheric imbalance in the exported EEG features, and to what extent might this reflect physiological dominance versus technical artifacts (e.g., electrode contact, reference montage, or channel scaling)?

4. Inter-Electrode Dependencies: What is the nature of the rank-based statistical correlations between different electrode channels across frequency bands, and how does this shared variance impact the interpretation of functional connectivity in exported feature summaries?

3. Research Design & Architectural Diagram

Below is the architectural flowchart of the research pipeline, illustrating the progression from data acquisition to spatial-spectral characterization and downstream BCI applications.

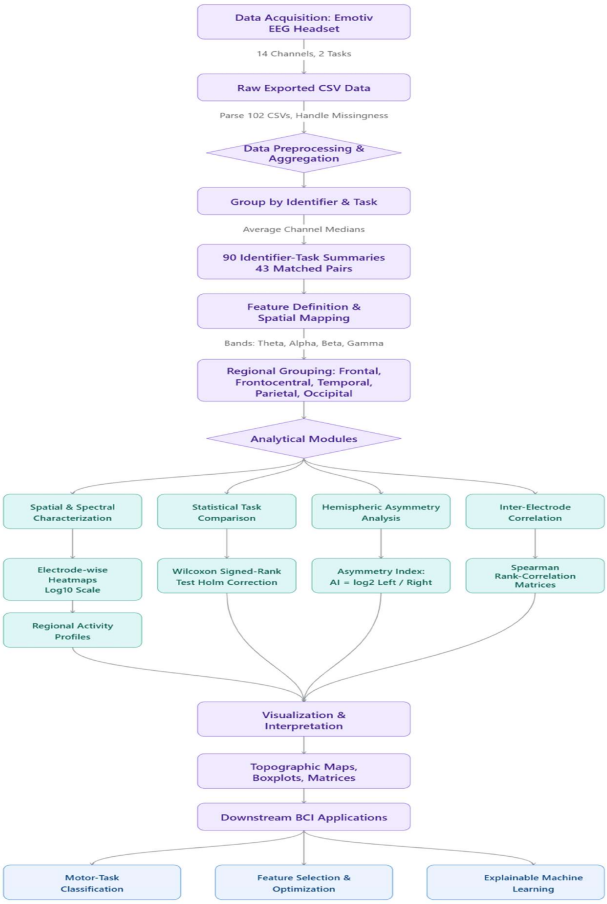

Figure 1. Architecture

3.1 Methodology

The methodology is structured into four primary phases: Data Preparation, Feature & Spatial Definition, Statistical Analysis, and Visualization.

3.2 Dataset Description and Preprocessing

• Data Source: The dataset consists of EEG recordings collected via an Emotiv EEG headset comprising 14 electrode locations (AF3, AF4, F3, F4, F7, F8, FC5, FC6, T7, T8, P7, P8, O1, O2).

• Experimental Tasks: Two motor-intention tasks were evaluated: LeftRight and PullPush.

• Data Consolidation: The archive contained 102 valid CSV files with exported frequency band features. Files sharing the same filename prefix (grouping identifier) and task were consolidated by averaging file level channel medians. This yielded 90 identifier-task summaries, with 43 matched identifiers available for paired LeftRight PullPush comparisons.

• Handling Skewness & Missingness: Due to extreme upper-tail values in the feature distributions, channel medians were utilized as the primary central tendency metric. Mean missingness across electrode feature cells was negligible (~0.03%).

2.3 Feature and Spatial Definitions

• Frequency Bands: Five exported features were analyzed: Theta, Alpha, BetaL (Low-beta), BetaH (High-beta), and Gamma. Total Beta was computed as the sum of BetaL and BetaH.

• Regional Grouping: Electrodes were aggregated into five scalp regions:

o *Frontal:* AF3, F7, F3, F4, F8, AF4

o *Frontocentral:* FC5, FC6

o *Temporal:* T7, T8

o *Parietal:* P7, P8

o *Occipital:* O1, O2

3.4 Statistical and Analytical Procedures

Task Specific Contrasts: To evaluate differences between LeftRight and PullPush tasks, paired Wilcoxon signed-rank tests were applied across the 43 matched identifiers. Holm correction was applied to control for the family wise error rate across multiple comparisons.

• Hemispheric Asymmetry: Laterality was quantified using a logarithmic left to right ratio: $AI = \log_2\left(\frac{L}{R}\right)$ Where L and R represent the feature measurements of homologous left and right electrode pairs (e.g., AF3-AF4, F3-F4). Positive values indicate left-side dominance; negative values indicate right side dominance.

• Inter Electrode Correlations: Spearman rank-correlation matrices were computed to assess monotonic relationships between electrode level feature summaries across recording identifiers. This approach was chosen over Pearson correlation to minimize the influence of extreme observations and non linear scaling artifacts.

3.5 Visualization and Interpretation Strategy

• Heatmaps: Utilized for electrode wise and regional comparisons on a $\log_{10}$ scale to accommodate skewed distributions and highlight relative feature magnitudes (e.g., identifying AF4 dominance in Theta/Alpha and FC6 dominance in Gamma).

• Boxplots: Deployed to illustrate between identifier variability, interquartile ranges, and right skewed distributions across predefined scalp regions.

• Topographic Mapping: Proposed as an interpolated spatial visualization to complement electrode wise data, providing an intuitive scalp level representation of frequency band activity (with the caveat that 14 channels limit precise cortical source localization).

3.6 Methodological Limitations & Caveats

• Feature-Level Analysis: The study relies on exported band power summaries rather than raw voltage time-series. Consequently, raw spectral estimation, artifact rejection, phase locking, and true functional connectivity (coherence) cannot be computed.

• Asymmetry Confounds: The consistent rightward asymmetry observed in the AI metric must be interpreted with caution, as it may stem from headset placement, impedance variations, or channel specific scaling rather than true physiological right hemisphere dominance.

• Metadata Constraints: Filename prefixes serve as grouping identifiers but are not independently verified human participant IDs; thus, cross participant generalization requires further acquisition metadata validation.

4. Dataset and processing

The archive contained 102 CSV files, all of which were parsed successfully. The files contained 14 electrodes and five exported frequency features. Filename prefixes yielded 47 distinct grouping identifiers. Multiple files sharing the same identifier and task were consolidated by averaging file level channel medians, resulting in 90 identifier task summaries: 46 LeftRight and 44 PullPush. Forty three identifiers had both tasks and were used for paired comparisons. Filename prefixes are grouping identifiers and are not independently verified human participant IDs.

Mean missingness across electrode feature cells was approximately 0.03%. The median recording contained about 1,679 rows and spanned about 210 seconds by timestamp. Channel medians were used because the feature distributions included extreme upper tail values.

The uploaded ZIP file contains an interesting EEG based brain computer interface (BCI) dataset collected using an Emotiv EEG headset. It is suitable for an integrated study involving EEG signal analysis, cognitive state recognition, motor imagery classification, machine learning, and brain activity pattern discovery.

The dataset appears particularly suitable for investigating whether EEG frequency band activity can distinguish between different motor intention tasks, especially left right and pull push movements.

4.1 Dataset structure and initial observations

We identified the following structure.

187 - Total files

102 - CSV files

85 - TXT log files

70 -EEG feature columns per valid CSV

Identified experimental tasks

• LeftRight

• PullPush

The CSV files contain:

Component	Description
Timestamp	Time associated with each observation
EEG electrodes	14 electrode locations
Theta	Theta-band power
Alpha	Alpha-band power
BetaL	Low-beta power
BetaH	High-beta power
Gamma	Gamma-band power

The 14 electrode locations include AF3, AF4, F3, F4, F7, F8, FC5, FC6, T7, T8, P7, P8, O1 and O2.

Each valid CSV therefore contains 70 EEG frequency-band features plus a timestamp.

Important initial observations:

• The CSV files appear to contain repeated measurements from multiple recording sessions or participants.

• Files are organized around the two experimental tasks.

• Some filenames have duplicate-looking versions, such as (1), which need investigation.

• Some files contain missing values or potentially malformed records.

• The TXT files contain acquisition and headset communication logs, which may help reconstruct recording metadata.

The timestamp intervals in the inspected CSV examples are approximately 0.125 seconds. This suggests an approximately 8 Hz feature-update interval, not necessarily the original EEG sampling frequency.

4.2 Feature and spatial definitions

The five supplied features were theta, alpha, betaL, betaH and gamma at AF3, F7, F3, FC5, T7, P7, O1, O2, P8, T8, FC6, F4, F8 and AF4. Beta was calculated as betaL + betaH; original sub-band values remain in the workbook.

Regional grouping: frontal (AF3, F7, F3, F4, F8, AF4); temporal (T7, T8); parietal (P7, P8); occipital (O1, O2); and frontocentral (FC5, FC6). FC5/FC6 were kept separate rather than assigned to one of the four lobar regions.

Paired Left Right PullPush comparisons used Wilcoxon signed rank tests across 43 matched identifiers, with Holm correction. Laterality was defined as log2(left channel/right channel); positive values indicate greater left side feature values and negative values indicate greater right side feature values.

5. Results

5.1 Electrode-wise and frequency-band patterns

AF4 had the highest median theta and alpha values in both tasks. AF4 was the highest median beta electrode in LeftRight, whereas FC6 was highest in PullPush. FC6 showed the highest median gamma values in both tasks. These are descriptive maxima and do not establish statistically localized cortical activation.

5.2 Regional activity

Frontal activity had the highest regional median for theta and alpha in both tasks. The highest beta median was frontocentral in LeftRight and frontal in PullPush. Frontocentral activity had the highest gamma median in both tasks. Frontal/frontocentral feature magnitudes were generally higher than temporal, parietal or occipital magnitudes.

5.3 Task-specific activation

Neither electrode wise nor regional paired task comparisons were statistically significant after Holm correction. Differences visible in the plots should therefore be treated as descriptive rather than confirmed task-specific activation effects.

5.4 Left right hemispheric asymmetry

Median log2(left/right) laterality indices were negative across all four bands in both tasks. Across homologous electrode pairs, median indices ranged approximately from -0.65 to -0.46 in LeftRight and -0.62 to -0.41 in PullPush. Several individual pair by band tests differed from zero after Holm correction, but task differences in laterality did not remain significant after correction.

The broadly rightward pattern across many pairs may reflect channel scaling, electrode contact, reference montage, headset placement or preprocessing effects. It should not be interpreted as physiological right-hemisphere dominance without independent signal quality checks and baseline normalization.

5.5 Inter-electrode correlations

Spearman correlations between electrode level summaries were predominantly positive. Mean pairwise correlations ranged from 0.565 to 0.701 in LeftRight and 0.570 to 0.665 in PullPush. Gamma had the highest mean pairwise correlation in both tasks. These are cross identifier correlations between exported features, not measures of coherence, phase synchronization or functional connectivity.

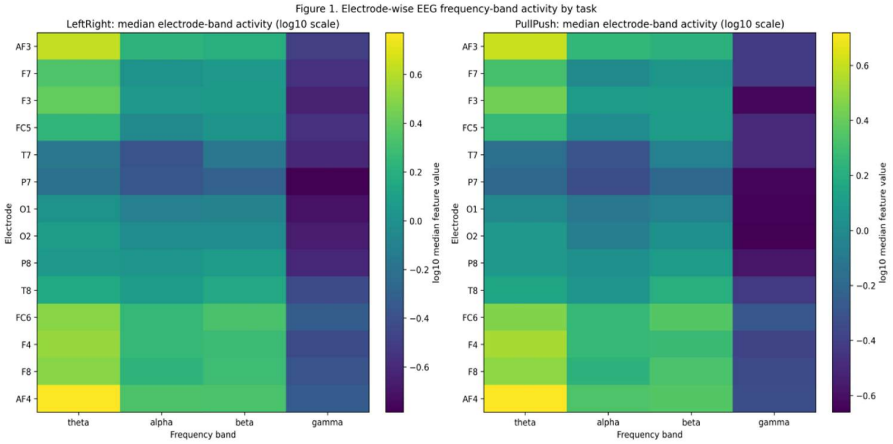

Figure 1. Electrode wise EEG frequency band activity by task

Heatmaps compare median feature values across electrodes and bands on a log10 scale. AF4 is prominent for theta and alpha; FC6 is prominent for gamma and PullPush beta.

Figure 1 illustrates the distribution of EEG frequency band activity across the 14 electrode locations under the LeftRight and PullPush experimental conditions. The visualization compares theta, alpha, beta and gamma activity across the frontal, temporal, parietal, occipital and frontocentral electrode locations. The heatmap provides a comparative representation of electrode specific feature magnitudes, allowing variations in frequency-band activity to be examined across the two motor tasks. The use of a logarithmic representation facilitates the visualization of differences in feature magnitude and accommodates the skewed distributions observed in the exported EEG measurements.

The electrode-wise distribution indicates that EEG activity is not uniformly distributed across the electrode locations. AF4 exhibits comparatively high median theta and alpha activity under both experimental conditions, suggesting that the exported frequency band features at this electrode have relatively greater magnitudes than those at several other locations. For beta activity, AF4 exhibits the highest median value during LeftRight, whereas FC6 exhibits the highest median during PullPush. FC6 also demonstrates comparatively high gamma activity under both tasks.

These observations indicate electrode dependent variations in EEG frequency-band characteristics. However, the observed differences should be interpreted as variations in scalp recorded feature magnitudes rather than definitive evidence of localized cortical activation. Differences in electrode contact, reference configuration and channel specific scaling may also contribute to the observed patterns.

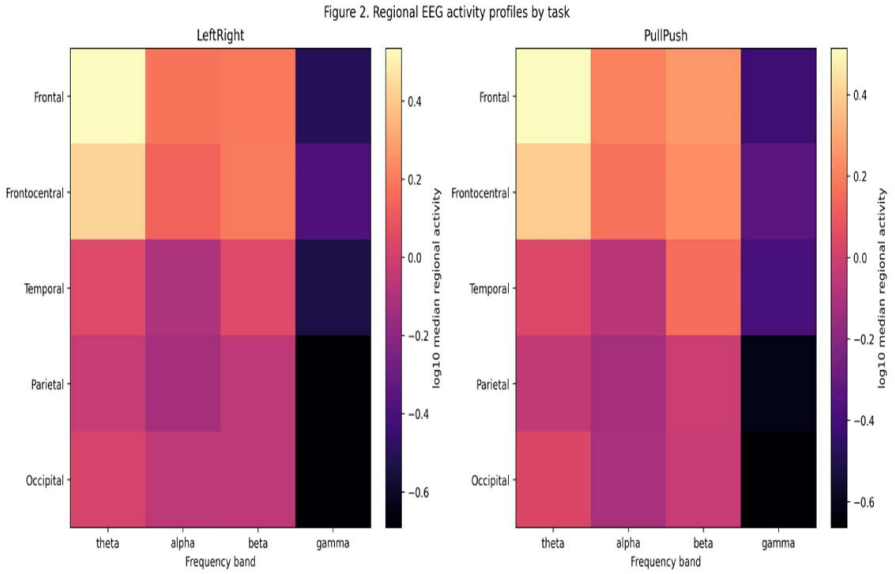

Figure 2. Regional EEG activity profiles by task

Regional heatmaps summarize frontal, frontocentral, temporal, parietal and occipital activity. Frontal sites dominate theta and alpha; frontocentral sites are prominent for gamma

Description

Figure 3 presents a regional comparison of EEG activity across frontal, frontocentral, temporal, parietal and occipital electrode groups. The regional representation is obtained by aggregating the electrode level measurements within each predefined scalp region. Separate comparisons are presented for the LeftRight and PullPush experimental tasks across the four principal frequency band families.

This visualization provides a higher-level spatial representation of EEG activity and facilitates the investigation

of regional variations that may not be immediately apparent from individual electrode measurements.

The regional distribution reveals relatively higher frontal activity for theta and alpha frequency bands under both experimental conditions. In contrast, beta activity exhibits a more differentiated spatial distribution, with frontocentral activity showing the highest regional median during LeftRight and frontal activity showing the highest median during PullPush. Gamma activity demonstrates comparatively higher frontocentral feature magnitudes under both tasks.

The results suggest that the spatial distribution of exported EEG frequency-band features varies according to frequency band and experimental condition. The relatively higher frontal theta and alpha values indicate that frontal electrode measurements contribute substantially to the overall regional feature distribution. Similarly, the higher frontocentral gamma values suggest that FC5 and FC6 contribute strongly to the observed gamma-band measurements.

Nevertheless, these findings are descriptive and should not be interpreted as evidence of statistically confirmed regional specialization.

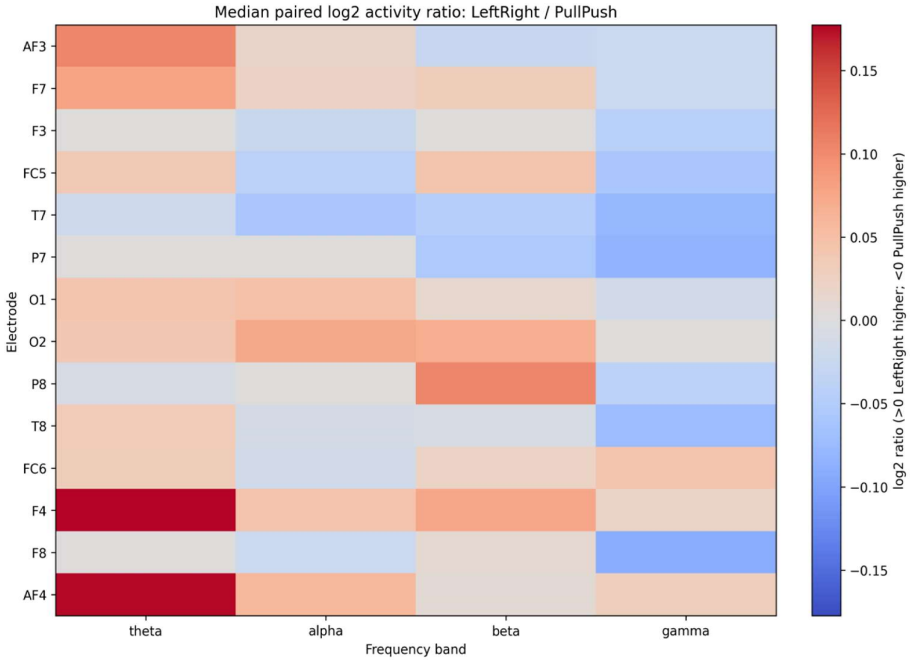

Figure 3. Task-Specific Electrode Activation Differences Between LeftRight and PullPush Conditions

Figure 4. Left–right hemispheric asymmetry
The heatmap shows the median paired log2 ratio of LeftRight to PullPush. Positive values indicate higher LeftRight values; negative values indicate higher PullPush values. Interpret alongside nonsignificant adjusted paired tests.

Figure 4 illustrates the electrode-specific differences in EEG frequency-band measurements between the LeftRight and PullPush motor tasks. The heatmap represents the median paired logarithmic ratio of the measurements obtained under the two experimental conditions for each electrode and frequency band.

Positive values indicate relatively higher feature measurements during the LeftRight task, whereas negative values indicate relatively higher measurements during the PullPush task. Values close to zero indicate relatively small differences between the two experimental conditions.

The paired comparison is based on 43 matched filename based recording identifiers, allowing the analysis to account for differences between matched recording groups rather than relying on independent comparisons of all individual observations.

The electrode specific contrast reveals variations in the magnitude and direction of EEG feature differences across the two experimental conditions. Certain electrode-frequency combinations exhibit relatively higher measurements during LeftRight, whereas others exhibit higher measurements during PullPush. These differences suggest that the two motor tasks may be associated with distinct patterns in the exported EEG frequency-band features.

However, the paired statistical analysis did not identify significant task specific differences after Holm correction. Consequently, the observed variations do not provide sufficient statistical evidence to establish reliable differences in electrode level activity between LeftRight and PullPush.

This finding is important because it distinguishes descriptive feature variations from statistically supported task related effects. It also indicates that additional analyses incorporating temporal EEG information, improved recording metadata and independent validation may be necessary to identify subtle motor task related patterns.

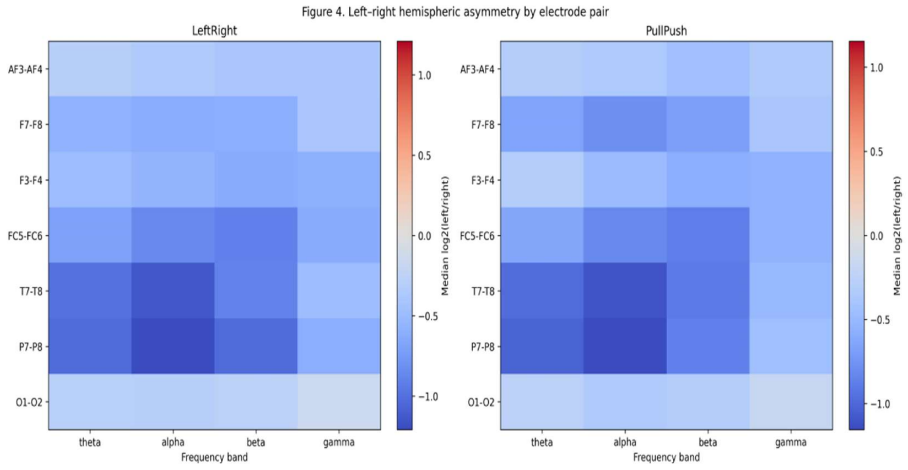

Figure 4. Left–right hemispheric asymmetry

Figure 4. Left–Right Hemispheric Asymmetry Across EEG Frequency Bands

Negative log2 (left/right) values dominate, indicating higher right side feature values. The consistency across pairs calls for technical validation before physiological interpretation.

Figure 5 presents the hemispheric asymmetry patterns observed across homologous electrode pairs under the LeftRight and PullPush experimental conditions. The analysis considers six corresponding electrode pairs: AF3–AF4, F3–F4, F7–F8, T7–T8, P7–P8 and O1–O2.

Hemispheric asymmetry is quantified using a logarithmic left to right ratio:

$$AI=\log_2\left(\frac{L}{R}\right)$$

where L and R represent the corresponding left and right side electrode feature measurements.

Positive asymmetry values indicate higher left side measurements, whereas negative values indicate higher right side measurements. The visualization enables the examination of whether the direction and magnitude of hemispheric asymmetry vary across frequency bands and experimental tasks.

The results demonstrate predominantly negative hemispheric asymmetry indices across the examined frequency bands and electrode pairs. The median asymmetry indices range approximately from -0.65 to -0.46 during LeftRight and from -0.62 to -0.41 during PullPush.

This consistent negative pattern indicates that right side electrode measurements generally exhibit higher feature magnitudes than their corresponding left side measurements. The pattern is observed across multiple scalp regions rather than being restricted to a single electrode pair.

The findings therefore suggest a systematic hemispheric imbalance in the exported EEG features. However, this observation requires careful interpretation because consistent asymmetry may also arise from electrode placement, contact quality, reference montage, channel calibration or preprocessing differences.

Accordingly, the observed rightward feature asymmetry should not be interpreted directly as right hemisphere functional dominance. Further validation using raw EEG recordings, signal quality measurements and appropriate baseline normalization would be necessary to establish its physiological significance.

Figure 5. Regional EEG activity distributions.
Log scale boxplots show between identifier variability and right skewed feature distributions. Medians and interquartile ranges are more robust summaries than arithmetic means.

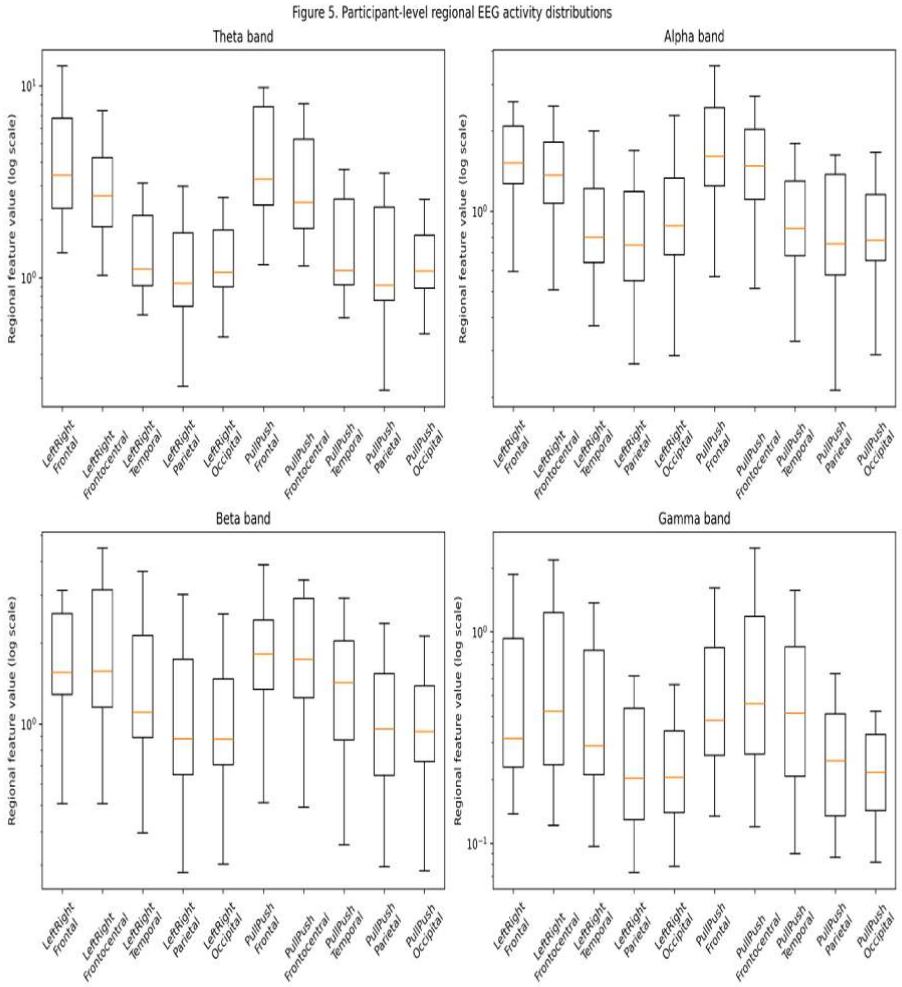

Figure 5. Regional Distribution and Variability of EEG Frequency-Band Measurements

Figure 6 presents the distribution of EEG frequency-band measurements across the predefined scalp regions using boxplots. Separate distributions are provided for the LeftRight and PullPush experimental conditions.

The boxplots summarize the median, interquartile range and variability of regional EEG measurements, while the whiskers and individual outlying observations provide additional information regarding the spread of the feature distributions.

The visualization enables comparisons of central tendency and variability across brain regions and frequency bands, providing information beyond the regional median comparisons presented in Figure 2.

The regional distributions indicate substantial variation in EEG feature magnitudes across recording identifiers. Frontal measurements generally demonstrate relatively higher theta and alpha feature values, whereas frontocentral measurements exhibit comparatively higher gamma activity.

The distributions also reveal differences in variability across regions and frequency bands. The presence of observations outside the central interquartile ranges indicates that EEG feature magnitudes vary considerably between recording groups. Such variability may reflect differences in individual physiological characteristics, recording conditions, electrode contact or experimental execution.

The relatively broad distributions emphasize the importance of using robust statistical summaries, including medians and interquartile ranges, when describing EEG frequency band measurements. They also indicate that regional differences should be examined alongside within region variability rather than being interpreted exclusively through mean or median values.

Overall, Figure 6 complements the regional heatmap by demonstrating the extent to which EEG activity measurements vary across the recording groups.

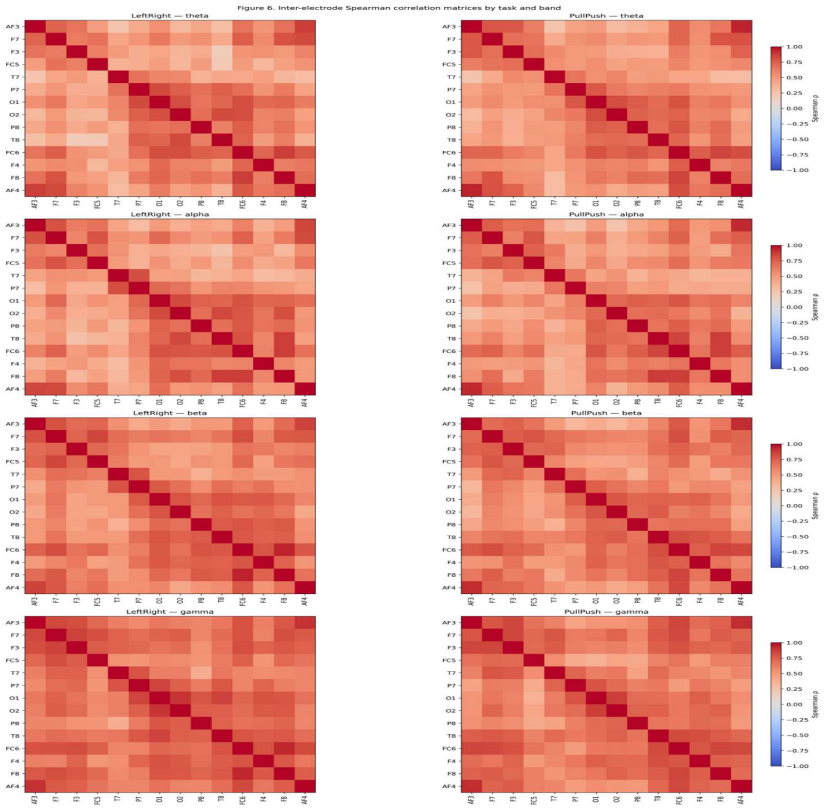

Figure 6. Inter-electrode Spearman correlation matrices

Figure 6. Inter-Electrode Spearman Correlation Matrices Across EEG Frequency Bands
Matrices show rank correlations between channel features by task and band. Positive associations are common, but these matrices do not quantify neural connectivity.

Figure 7 presents Spearman rank-correlation matrices describing the relationships between EEG feature measurements recorded at different electrode locations. Separate correlation matrices are generated for theta, alpha, beta and gamma frequency bands under the LeftRight and PullPush experimental conditions.

Each matrix represents the strength and direction of association between pairs of electrode level feature summaries across the recording identifiers. Positive correlation coefficients indicate that higher measurements at one electrode tend to be associated with higher measurements at another electrode. Negative coefficients indicate inverse relationships.

Spearman correlation is employed because it assesses monotonic relationships and is less sensitive to extreme observations than conventional Pearson correlation.

The correlation matrices reveal predominantly positive associations between electrode measurements across the investigated frequency bands and experimental conditions. The average pairwise Spearman correlation ranges from approximately 0.565 to 0.701 during LeftRight and from approximately 0.570 to 0.665 during PullPush.

Among the frequency bands, gamma exhibits the highest average pairwise correlation in both conditions, with mean correlation coefficients of approximately 0.701 and 0.665, respectively.

These findings suggest that EEG feature magnitudes across different electrode locations frequently exhibit similar variations across the recording groups. The positive associations may reflect shared variations in overall signal magnitude, common recording characteristics or coordinated changes in the exported frequency-band features.

Nevertheless, these correlations should not be interpreted as direct evidence of functional brain connectivity. The analysis is based on correlations between recording-level feature summaries and does not measure temporal synchronization, phase relationships or frequency-domain coherence between EEG signals.

Further investigation using raw EEG time series and established connectivity measures would be required to determine whether the observed associations correspond to underlying neural interactions.

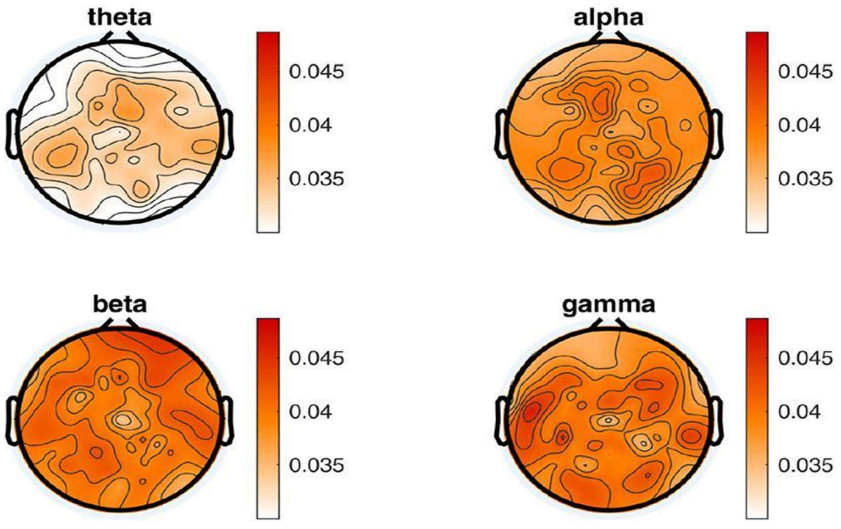

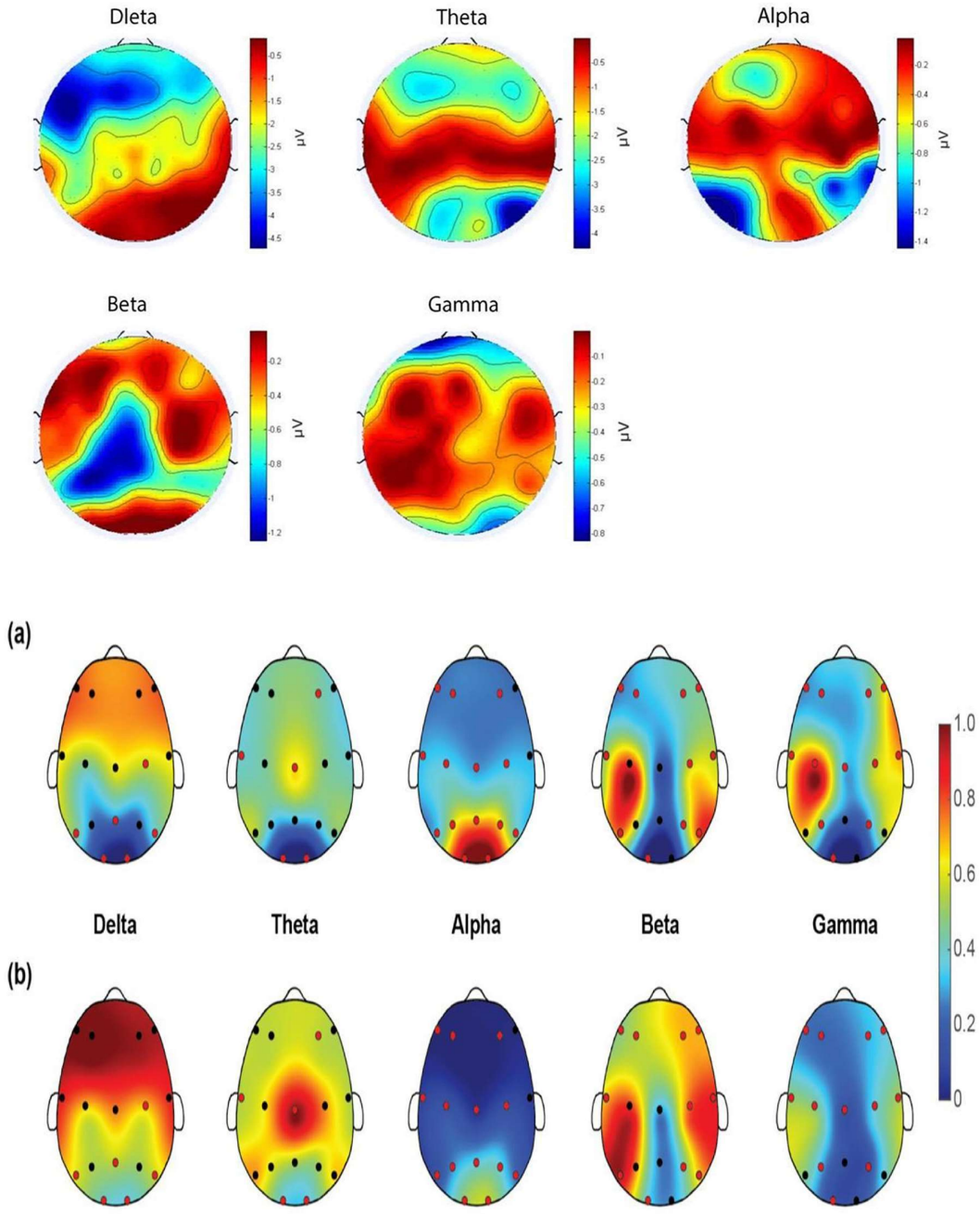

Figure 7. Scalp Topographic Distribution of EEG Frequency-Band Activity

Figure 7 is proposed as a complementary spatial visualization of EEG frequency band activity across the scalp. Separate topographic representations can be generated for theta, alpha, beta and gamma measurements under the LeftRight and PullPush experimental conditions. The spatial interpolation of electrode level measurements provides a continuous visual representation of the distribution of exported EEG feature magnitudes across the scalp.

The topographic representation would provide an intuitive means of examining spatial differences in EEG frequency band measurements between the two motor tasks. It could help identify whether the higher frontal theta and alpha values and frontocentral gamma values identified in the electrode wise and regional analyses

are also apparent in the overall spatial distributions.

However, the topographic maps should be considered interpolated visualizations of scalp electrode measurements. Given the limited 14-channel electrode configuration, they cannot establish precise cortical source locations or demonstrate the anatomical origin of the measured activity.

All the figures represented above provide complementary evidence concerning the spatial and frequency-band characteristics of EEG measurements during Left Right and Pull Push motor tasks. The electrode wise and regional analyses indicate that EEG feature magnitudes vary across scalp locations, with relatively higher frontal theta and alpha measurements and frontocentral gamma measurements. The task specific comparisons reveal descriptive variations between the experimental conditions, although these differences were not statistically significant following multiple comparison correction.

The hemispheric asymmetry analysis identifies a consistent tendency toward higher right side feature magnitudes across several homologous electrode pairs. This systematic pattern warrants additional technical investigation before physiological interpretations are made. Furthermore, the inter electrode correlation analysis demonstrates predominantly positive associations across the four frequency band families, suggesting that electrode level feature measurements exhibit shared variation across recording groups.

Collectively, these findings establish an initial spatial and spectral characterization of the supplied EEG dataset. They also provide a statistical foundation for subsequent motor task classification, feature selection and explainable machine learning investigations. Importantly, the results indicate that EEG feature distributions alone do not yet establish reliable differences between the two motor tasks, high lighting the need for leakage-controlled predictive validation and further examination of recording quality.

6. Discussion

6.1 Overview of principal findings

This work set out to characterize how exported EEG frequency band features are distributed across recording sites during two motor intention tasks, and to examine three complementary dimensions: electrode wise variation, hemispheric asymmetry, and inter electrode correlation. The analysis produced a coherent descriptive picture anterior dominance of theta and alpha, frontocentral prominence of gamma, a broadly rightward feature asymmetry, and widespread positive covariation between channels but it did not produce statistically confirmed differences between the LeftRight and PullPush conditions after correction for multiple comparisons. This dissociation between visible descriptive structure and absent inferential support is the central message of the study, and it is reported deliberately rather than treated as an incidental negative result.

6.2 Spatial and spectral organization of exported features

The electrode wise and regional analyses consistently identified anterior channels as carrying the largest feature magnitudes. AF4 exhibited the highest median theta and alpha values under both tasks, and frontal aggregates exceeded temporal, parietal and occipital aggregates for these bands. FC6 exhibited the highest median gamma under both conditions, and frontocentral aggregates dominated the gamma band. Beta showed a less stable spatial maximum, shifting from AF4/frontocentral in LeftRight to FC6/frontal in PullPush.

Two interpretations must be held simultaneously. First, anterior theta and fronto central high frequency activity are broadly consistent with the involvement of frontal and sensori motor adjacent regions in movement preparation and intention, which motivated the study. Second and importantly the analysis operates on exported band power summaries whose physical units, calibration and internal preprocessing are undocumented. Consequently, an electrode with a large median feature value is not equivalent to a cortical generator with high activity. Reference montage configuration, electrode scalp impedance, headset fit and channel specific gain can all elevate one site relative to another without any corresponding difference in neural activity. The descriptive maxima reported here are therefore properties of the *exported feature scale at the scalp*, not evidence of localized cortical activation.

6.3 Absence of statistically confirmed task effects

Paired Wilcoxon signed rank comparisons across 43 matched identifiers yielded no electrode wise or regional differences that survived Holm correction. Several considerations bear on the interpretation of this null result. The contrast heatmaps (Figure 4) do show non zero median paired log, ratios, indicating that the two tasks differ in the direction and magnitude of feature values in a descriptive sense. However, these deviations are small relative to the between identifier variability documented in the regional boxplots (Figure 6), where interquartile ranges span wide intervals, and numerous observations fall outside the whiskers. When between recording variability substantially exceeds within recording task effects, paired non parametric tests on a moderate number of identifiers have limited power, particularly under family wise error control across many electrode band combinations.

Three non exclusive explanations follow. (i) The two tasks may genuinely produce highly overlapping spectral signatures at the level of aggregated band power, with any discriminative information residing in temporal dynamics, event related desynchronization/synchronization timing, or spatial patterns that median aggregation removes. (ii) Discriminative information may exist but be obscured by the loss of temporal structure inherent in collapsing an approximately 210-second recording (≈ median 1,679 rows at ≈ 0.125 s intervals) into a single per channel median. (iii) Effect sizes may be small enough that the present sample of matched identifiers is insufficient to detect them under conservative correction. The present data cannot adjudicate among these possibilities, and the appropriate conclusion is that task specific activation differences were not established, not that they were shown to be absent.

6.4 Hemispheric asymmetry: physiological or technical

Median log, (left/right) indices were negative across all four band families and both tasks, with values ranging from approximately -0.65 to -0.46 in LeftRight and -0.62 to -0.41 in PullPush. Several individual pair by band tests differed from zero after Holm correction, whereas task related differences in laterality did not survive correction.

The critical feature of this result is its breadth and consistency. A physiologically motivated lateralization associated with, for example, right hand motor intention would be expected to show regional specificity concentrated over sensorimotor adjacent pairs and task dependence. Instead, the rightward offset appears across frontal, temporal, parietal and occipital pairs, across all bands, and in both tasks with similar magnitude. A spatially and spectrally global offset of this kind is more parsimoniously explained by a systematic measurement factor: asymmetric headset placement, differing electrode contact quality between hemispheres, reference channel positioning, or channel-level scaling in the export pipeline. Accordingly, the observed asymmetry is reported as a property of the recorded feature set requiring technical validation, and is explicitly not interpreted as right hemisphere functional dominance. Baseline normalization, impedance logging and independent signal quality assessment are prerequisites for any physiological reading of this pattern.

6.5 Inter-electrode correlations and shared variance

Spearman correlations between electrode-level summaries were predominantly positive, with mean pairwise coefficients of 0.565–0.701 (LeftRight) and 0.570–0.665 (PullPush); gamma exhibited the highest mean correlation in both tasks. These are correlations of *recording level summary values across identifiers*, not time resolved measures of neural coupling. They therefore cannot be equated with coherence, phase-locking value, phase synchronization, or functional connectivity, and the manuscript consistently avoids that terminology.

Substantively, correlations of this magnitude imply that a large fraction of the variance in the 70-dimensional feature space is shared. This has direct methodological consequences. First, the effective dimensionality of the feature set is far lower than its nominal dimensionality, so treating channels as independent predictors overstates the information available. Second, strongly correlated features inflate apparent model performance when feature selection or normalization is performed outside a properly nested cross validation scheme. Third, a global covariation component plausibly reflecting overall signal gain, arousal, session level recording conditions or export scaling is a plausible driver of both the positive correlations and the uniform asymmetry offset,

linking the two findings to a common technical origin.

6.6 Implications for BCI-oriented modelling

Taken together, the results argue for a cautious progression from characterization to prediction. The descriptive maps provide a defensible starting point for hypothesis generation and for restricting candidate feature subsets, but they do not license claims of task decoding. Any subsequent classification study on this archive should (i) enforce identifier-level grouping in all data splits to prevent leakage across recordings sharing a filename prefix, (ii) apply dimensionality reduction or regularization appropriate to highly collinear inputs, (iii) report performance against a permutation-based chance baseline, and (iv) accompany accuracy figures with attribution analyses that are checked against the possibility that the model has learned channel gain or session identity rather than motor intention.

6.7 Limitations and future directions

Several constraints bound the present conclusions. The archive contains exported band-feature summaries rather than raw voltage time series, so spectral re-estimation, artifact rejection, connectivity estimation and source localization are not possible. The physical units and calibration of the exported features are undocumented, and values are reported in the supplied feature scale. Filename prefixes function as grouping identifiers but are not verified participant identities, limiting any claim of cross participant generalization; the 85 accompanying TXT acquisition logs may allow reconstruction of session metadata and partial resolution of this issue. Duplicate-looking filenames require adjudication: if such files represent independent runs rather than duplicate exports, a run-level hierarchical model would preserve that structure and alter the effective sample size. Finally, the 14-channel montage supports interpolated scalp visualization (Figure 8) but not anatomical source inference.

Priority next steps are therefore: recovery of raw EEG for principled preprocessing and connectivity analysis; extraction of event locked, time resolved features rather than whole recording medians; documentation of impedance, reference and export calibration; verification of participant and session metadata; and adequately powered, leakage controlled predictive validation.

7. Conclusion

This study provides a systematic spatial and frequency-band characterization of exported EEG features recorded with a 14-channel Emotiv headset during LeftRight and PullPush motor intention tasks. Across 90 identifier–task summaries derived from 102 valid recordings, feature magnitudes were reliably non-uniform across the scalp: AF4 carried the highest median theta and alpha values, FC6 the highest median gamma, frontal regions dominated theta and alpha, and frontocentral regions dominated gamma. These spatial patterns were stable across both tasks and are reported on a logarithmic scale to accommodate strongly right skewed feature distributions.

Three findings qualify any stronger interpretation. First, no electrode-wise or regional paired task comparison reached statistical significance after Holm correction, so the visible differences between conditions remain descriptive. Second, hemispheric asymmetry indices were uniformly negative across bands, tasks and homologous electrode pairs, a globally consistent offset that is more consistent with montage, contact or channel-scaling effects than with lateralized cortical function. Third, inter electrode Spearman correlations were predominantly positive and substantial, indicating considerable shared variance and reduced effective dimensionality; these associations are properties of recording-level feature summaries and are not measures of neural connectivity.

The contribution of this work is therefore a transparent, reproducible descriptive baseline together with an explicit account of what the available data can and cannot support. Exported band power summaries alone do not, on this evidence, establish reliable discrimination between the two motor tasks, nor physiological hemispheric dominance. By documenting these boundaries rather than overstating the descriptive patterns, the study defines a concrete agenda for subsequent work signal-quality verification, recovery of raw time

series, metadata validation and leakage controlled predictive modelling that must be completed before spatial–spectral EEG features can be advanced as dependable control signals for assistive and rehabilitation oriented brain computer interfaces.

References

[1] Yahya, N., Musa, H., Ong, Z. Y., Elamvazuthi, I. (2019). Classification of motor functions from electroencephalogram (EEG) signals based on an integrated method comprised of common spatial pattern and wavelet transform framework. *Sensors, 19*(22), Article 4878. https://doi.org/10.3390/s19224878.

[2] Chen, J., Xia, Y., Zhou, X., Vidal Rosas, E., Thomas, A., Loureiro, R., et al. (2023). fNIRS-EEG BCIs for motor rehabilitation: A review. *Bioengineering, 10*, Article 1393. https://doi.org/10.3390/bioengineering10121393

[3] Gao, N., Chen, P., Liang, L. (2023). BCI-VR-based hand soft rehabilitation system with its applications in hand rehabilitation after stroke. *International Journal of Precision Engineering and Manufacturing, 24*, 1403–1424. https://doi.org/10.1007/s12541-023-00835-2.

[4] Chen, X., Zhao, B., Wang, Y., Gao, X. (2019). Combination of high-frequency SSVEP-based BCI and computer vision for controlling a robotic arm. *Journal of Neural Engineering, 16*, Article 026012. https://doi.org/10.1088/1741-2552/aaf594.

[5] Li, M., Li, F., Pan, J., Zhang, D., Zhao, S., Li, J., et al. (2021). The MindGomoku: An online P300 BCI game based on Bayesian deep learning. *Sensors, 21*, Article 1613. https://doi.org/10.3390/s21051613.

[6] Deng, T., Huo, Z., Zhang, L., Dong, Z., Niu, L., Kan/. M,MMg, X., et al. (2023). A VR-based BCI interactive system for UAV swarm control. *Biomedical Signal Processing and Control, 85*, Article 104944. https://doi.org/10.1016/j.bspc.2023.104944.

[7] Wu, J., Wang, J. (2024). An analysis of traditional methods and deep learning methods in SSVEP-based BCI: A survey. *Electronics, 13*, Article 2767. https://doi.org/10.3390/electronics13142767.

[8] Yin, E., Zhou, Z., Jiang, J., Yu, Y., Hu, D. (2014). A dynamically optimized SSVEP brain computer interface (BCI) speller. *IEEE Transactions on Biomedical Engineering, 62*, 1447–1456. https://doi.org/10.1109/TBME.2014.2320948.

[9] Yin, E., Zhou, Z., Jiang, J., Chen, F., Liu, Y., Hu, D. (2013a). A novel hybrid BCI speller based on the incorporation of SSVEP into the P300 paradigm. *Journal of Neural Engineering, 10*, Article 026012. https://doi.org/10.1088/1741-2560/10/2/026012.

[10] Yin, E., Zhou, Z., Jiang, J., Chen, F., Liu, Y., Hu, D. (2013b). A speedy hybrid BCI spelling approach combining P300 and SSVEP. *IEEE Transactions on Biomedical Engineering, 61*, 473–483. https://doi.org/10.1109/TBME.2013.2281976.

[11] Al-Saegh, A., Dawwd, S. A., Abdul Jabbar, J. M. (2021). Deep learning for motor imagery EEG-based classification: A review. *Biomedical Signal Processing and Control, 63*, Article 102172. https://doi.org/10.1016/j.bspc.2020.102172.

[12] Li, X., Chu, Y., Wu, X. (2024). 3D convolutional neural network based on spatial spectral feature pictures learning for decoding motor imagery EEG signal. *Frontiers in Neurorobotics, 18*, Article 1485640. https://doi.org/10.3389/fnbot.2024.1485640.

[13] Gu, Y., Dremstrup, K., Farina, D. (2009). Single trial discrimination of type and speed of wrist movements from EEG recordings. *Clinical Neurophysiology, 120*, 1596–1600.

[14] Liao, K., Xiao, R., Gonzalez, J., Ding, L. (2014). Decoding individual finger movements from one hand using human EEG signals. *PLoS ONE, 9*, Article e85192.

[15] Li, T., Xue, T., Wang, B., Zhang, J. (2018). Decoding voluntary movement of single hand based on analysis of brain connectivity by using EEG signals. *Frontiers in Human Neuroscience, 12*.

[16] Zhou, J., Yao, J., Deng, J., Dewald, J. (2009). EEG based classification for elbow versus shoulder torque intentions involving stroke subjects. *Computers in Biology and Medicine, 39*, 443–452.

[17] Úbeda, A., Azorin, J., Chavarriaga, R., Millan, J. d. R. (2017). Classification of upper limb center out reaching tasks by means of EEG based continuous decoding techniques. *Journal of NeuroEngineering and Rehabilitation, 14*.

[18] Juan, J. V., Pacheco, S., Iáñez, E., Ortiz, M., Tornero, J., Azorín, J. M. (2025). Improving motor imagery decoding through EEG frequency band analysis. In *2025 IEEE International Conference on Metrology for eXtended Reality, Artificial Intelligence and Neural Engineering (MetroXRAINE)* (p. 1107–1112). IEEE. https://doi.org/10.1109/MetroXRAINE66377.2025.11340400.

[19] Shang, Y., Gao, X., An, A. (2023). Multi-band spatial feature extraction and classification for motor imaging EEG signals based on OSFBCSP GAO SVM model. *Medical Biological Engineering Computing, 61*, 1581–1602. https://doi.org/10.1007/s11517-023-02793-3.

[20] Li, Q., Huang, J., Zhou, H. (2026). SC-SDT: A framework with spectral convolution and spatial differential transformer for EEG-based emotion recognition. *Cognitive Neurodynamics, 20*, Article 26. https://doi.org/10.1007/s11571-025-10394.

[21] Das, M., Pal, P., Mahadevappa, M. (2026). Detection of ASD using DySTEP-GAT architecture with EEG-based attention fused brain net graph representation. *IEEE Transactions on Instrumentation and Measurement, 75*, Article 4013112. https://doi.org/10.1109/TIM.2026.3716462.

[22] Kostoglou, K., Müller Putz, G. R. (2026). Opposing cortical forces: Alpha slowing and sensorimotor mu acceleration during motor related BCI training. *PLOS Computational Biology, 22*(4), Article e1014112.

[23] Kumar, J. S., Bhuvaneswari, P. (2012). Analysis of electroencephalography (EEG) signals and its categorization A study. *Procedia Engineering, 38*, 2525–2536.